Available online at www.sciencedirect.com
ScienceDirect
Journal of Nuclear Materials 366 (2007) 1–7
journal of nuclear materials
www.elsevier.com/locate/jnucmat

In situ observation of interfacial fatigue crack growth in diffusion bonded joints of austenitic stainless steel

Shu-xin Li, Fu-Zhen Xuan, Shan-Tung Tu *

School of Mechanical and Power Engineering, East China University of Science and Technology, 130, Meilong Road, P.O. Box 402, Shanghai 200237, PR China

Received 14 August 2006; accepted 14 December 2006

Abstract

Micro-fatigue tests were performed on 316LSS vacuum diffusion bonded joints to investigate the interfacial fatigue crack growth behavior with discrete micro-voids located ahead of a pre-existing crack tip. In situ observation of the interfacial fatigue crack propagation and micro-voids evolution was carried out during the whole fatigue testing. SEM of the fracture surface was analyzed. The results showed that the interface failure mechanism of similar diffusion bonded joints is different from that of dissimilar materials joints. A brittle mode is observed in the main crack growth. And the ridge interface formed in diffusion bonded joints due to surface roughness can be a resistance to the crack growth. The location of the fatigue crack initiation and the crack propagation direction derived from SEM observation of the fracture surface of the specimen are in consistent with those obtained from the in situ observation by using the optical microscope.

1. Introduction

As one of the advanced material joining techniques, diffusion bonding has been gaining greater attention in the fabrication of complicated and compacted structures. For example, the first wall and divertor components of international thermonuclear experimental reactor (ITER) are made of diffusion bonded stainless steel (SS) plates and Cu-alloy bonded to SS [1]. Diffusion bonding techniques were also applied to manufacture a compact intermediate heat exchanger for next-generation high temperature gas-cooled reactor [2].

To ensure the reliability of components sealed by diffusion bonding, many works have been carried out on the diffusion bonded joints of alloy-316LNSS or alloy-304SS [3–8]. In these studies, the strength of bonded joints was evaluated by tensile and shear strength. Only a limited number of studies on fatigue behavior of diffusion bonded joints of austenitic stainless steel have been openly reported. Nishi [9,10] studied the fatigue fracture behavior on diffusion bonded joints of alumina dispersion-strengthened copper (DSCu) to 316SS both experimentally and theoretically. The fracture location for the joint specimens varied with the strain distribution.

* Corresponding author. Tel.: +86 21 64253425; fax: +86 21 64253513.
E-mail addresses: li_shuxion@163.com (S.-x. Li), sttu@ecust.edu.cn (S.-T. Tu).

0022-3115/$ - see front matter © 2007 Published by Elsevier B.V.
doi:10.1016/j.jnucmat.2006.12.026

A good agreement was observed between the measured and predicted results. To provide the optimum bonding condition for hot isostatic pressing (HIP) bonded joints of 316LSS and DSCu, tensile and fatigue tests were conducted on the joints by Sato et al. [11]. Marois et al. [12] also discussed the joining of 316LSS to DSCu by HIP. The joint quality was assessed by tensile and fatigue testing at room temperature and 300 °C.

However, the earlier studies focused on the dissimilar joints of austenitic stainless steel. Although the fatigue properties of similar joints 316SS/316SS were discussed by Sato et al. [1], the diffusion bonding condition was constrained on the HIP. Furthermore, micro-voids left on bonded interface will influence the behavior of fatigue crack propagation, but the investigation of how those micro-voids influence the fatigue crack growth of similar diffusion bonded joints has not been carried out yet. As for in situ observation of interfacial crack growth, Lin et al. [13], Tanaka et al. [14] and Zhu et al. [15] have conducted experimental researches on dissimilar joints of SiC-fiber/Sic and SCS-6/Ti-15-3 composite. However, to date, no in situ observation of the interfacial fatigue crack growth in diffusion bonded joints of austenitic stainless steel was reported.

In this study, the similar austenitic stainless steel joints were bonded by vacuum diffusion bonding. The in situ observation of the fatigue crack growth was carried out by applying a newly-designed micro-fatigue testing device. Both the evolution of the interfacial crack and micro-voids can be monitored during the whole fatigue testing process, which provides us sufficient information to interpret the failure mechanism of the similar diffusion bonded joints on micro-scale.

2. Experimental procedures

2.1. Specimen preparation

The material used in this study was cold-worked 316LSS having the following chemical composition in wt%: C – 0.01, Si – 0.41, Mn – 1.41, P – 0.036, S – 0.006, Ni – 12.43, Cr – 17.84, Mo – 2.16, Fe – balance. The joining was carried out in a vacuum diffusion bonding equipment with a vacuum of 1.33×10^{-3} Pa. In order to optimize the three main joining parameters (temperature, pressure and time), a series of diffusion bonding tests were conducted under the conditions of temperature 1050–1100 °C, pressure 7–10 MPa and holding time 2–5 h. Tensile tests and Charpy impact at room temperature were carried out after bonding. The results showed that the good joint was obtained with the temperature 1100 °C (80% T_m, 316LSS melting temperature $T_m \approx 1370$ °C), pressure 10 MPa and the holding time 3 h.

After joining, detailed metallographic inspections were made along the bonding line. It was showed that the percentage of bonded area is more than 90%. Three repeated tensile test were conducted with the average ultimate tensile strength 566 MPa (about 93.6% σ_{b1}, σ_{b1} is the ultimate tensile strength of parent material), yield strength 210 MPa and section shrinkage rate ψ 28%. The repeatability in the mechanical response was good with only minor variations.

Single edge-notched fatigue specimen was employed in the fatigue testing. The specimen was manufactured with notch at the interface, shown in Fig. 1. The specimen was ground and polished to obtain their appearance of metallographic structure. For joints of similar materials with high percentage of bonded area, the interface can only be visible under microscope. So the accuracy of dimension A is very important in mechanical machining of the notch. Any minor error will lead to the notch deviation from the interface.

2.2. Fatigue testing system

A new testing system was developed to perform the in situ observation of interfacial crack growth of 316LSS/316LSS joints under cyclic loading. It consists of three main parts: loading system, supporting platform and data-collecting system, shown in Fig. 2. The system is used for small specimens (section area 3 mm × 3 mm or 3 mm × 1 mm). It possesses a number of merits such as compactness,

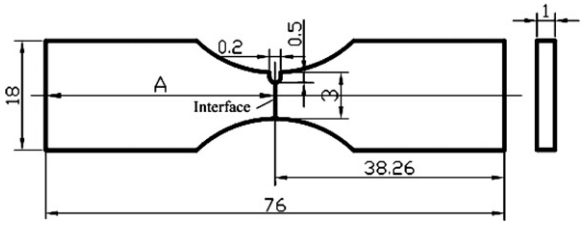

Fig. 1. Shape and dimensions of the single edge-notched fatigue specimen (mm).

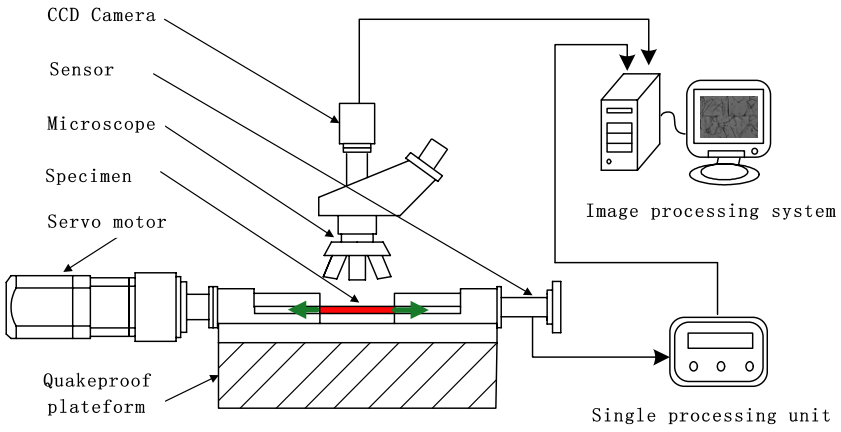

Fig. 2. Schematic diagram of the microscopic fatigue test system.

little vibration and low noise. The controlling software is programmed by LabVIEW.

2.3. Micro-fatigue testing

The fatigue tests were performed at room temperature under load control at $R = 0.1$, with a sine waveform of 0.5 Hz frequency. The axial tension–tension loading was perpendicular to the interface. The test was paused after a number of cycles in order to take and save pictures, with the load holding at the average stress, and then restarted. The maximum load amplitude is 500 N (215MP, 38% σ_{b2}, σ_{b2} is the ultimate tensile strength of joints).

3. Results and discussion

3.1. Interfacial fatigue crack initiation and propagation

In the fatigue test, the maximum stress level is close to the yield strength of the joint. So slip lines were found in grains at the notch after 1500 cycles. The slip lines were orientated along maximum shear stress direction. These slip lines became denser and new slip lines formed with increasing cycles, shown in Fig. 3, cycles $N = 3000$ and $N = 10\,000$. As the fatigue test proceeded, the slip lines in which crack initiated were strengthened continuously until the crack finished initiating and began to propagate.

Fig. 4 shows the evolution of the interfacial crack and micro-voids from 20 000 cycles to 30 000 cycles. The fatigue life of this specimen is 30 350 cycles. For clear interpretation, cracks and micro-voids were labeled with capital letters in Fig. 4 since there is more than one crack produced in the fatigue loading, with the main crack labeling A. Crack initiated at the upper side of the interface. When the cycles reached 20 000, the crack has grown 0.006 mm and advanced towards the interface in 60° direction with the interface, shown in Fig. 4(a) ($N = 20\,000$). The crack proceeded until the crack tip met the interface. Then it coalesced with the micro-void B, developing the main crack A, Fig. 4(b) ($N = 22\,175$).

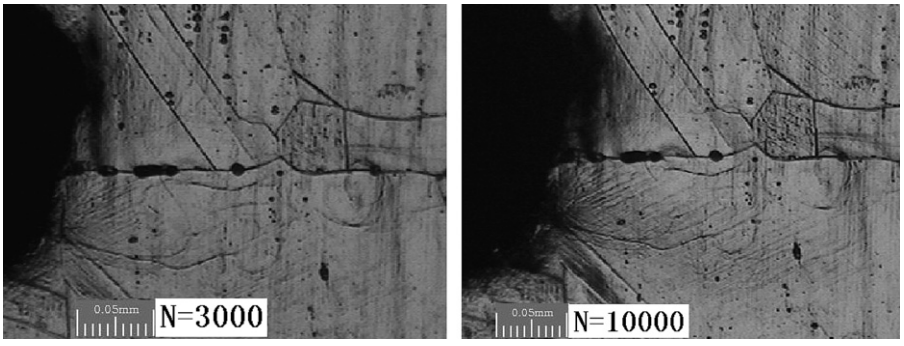

Fig. 3. Slip lines in grains at the notch under fatigue loading.

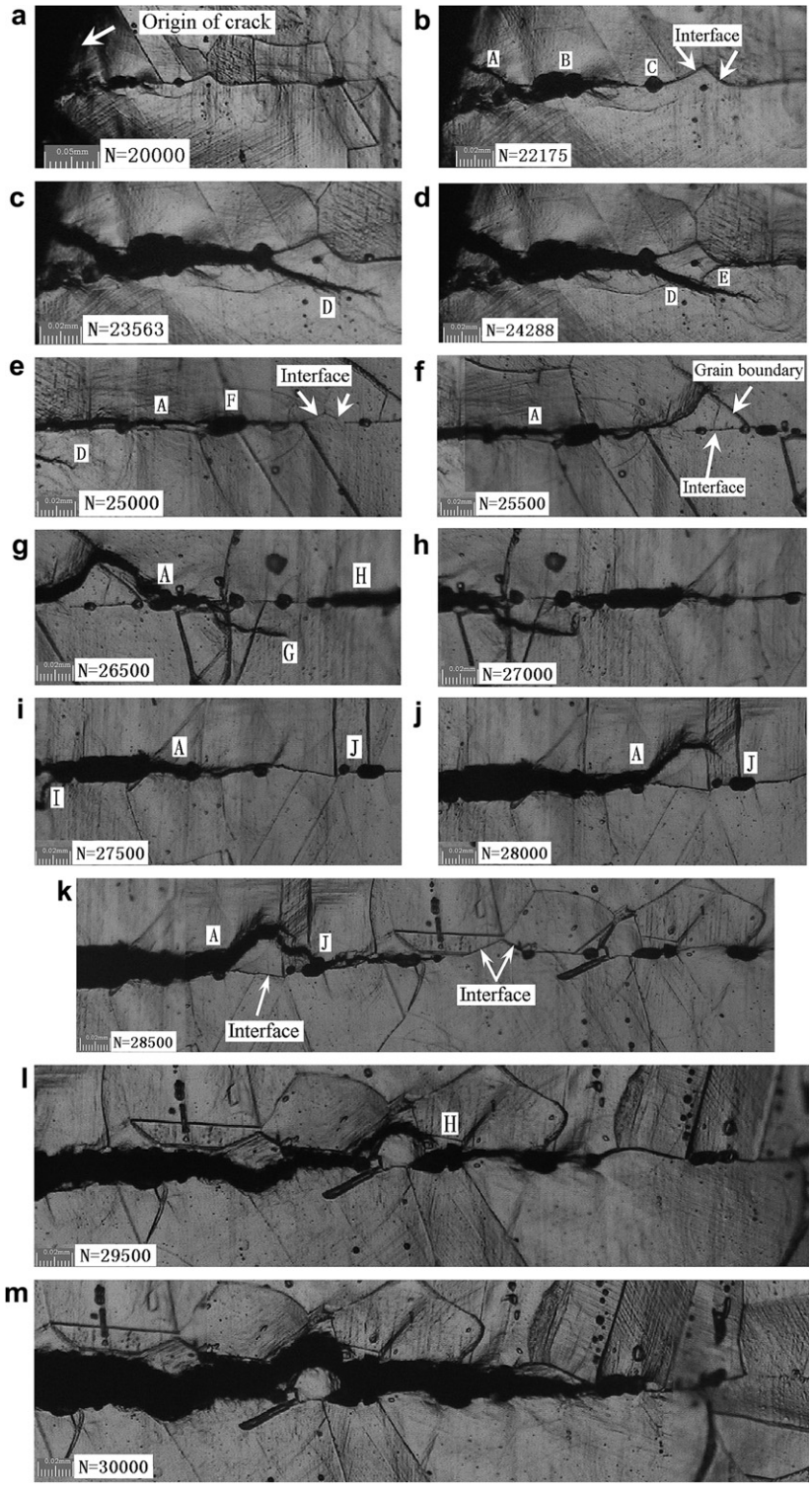

Fig. 4. Evolution of the interfacial fatigue crack and micro-voids at the bonded interface.

The interface ahead of the micro-void C is ridge-like rather than straight, Fig. 4(b). In diffusion bonding, a ridge interface is formed when the two convex surfaces contact. The size of ridge is therefore

determined by the surface roughness. The main crack did not propagate along the interface after it passed through the micro-void C. Instead, it changed the direction and grew on the symmetrically opposite direction of ridge, forming the crack D, shown in Fig. 4(c) ($N = 23\,563$). The crack D seemed to become the main crack. However, a new crack E produced at the symmetric location of the right side of ridge and grew towards the interface, Fig. 4(d) ($N = 24\,288$). In subsequent propagation it became the main crack. Meanwhile, the crack E stopped propagating and arrested at the grain, Fig. 4(e) ($N = 25\,000$). It is worth noting that, in this region, the crack became transgranular rather than propagated along the interface. As the crack extended, the crack coalesced with the micro-void F immediately, causing a jump-like increase in the crack length, which accelerated the crack growth process.

It can be seen in Fig. 4(f) ($N = 25\,500$) that the main crack extended along the left side of ridge interface, but impeded by the grain boundary ahead. In fact, the ridge interface can resist the crack propagation, namely reduces crack propagation rate to a certain degree. The reason is probably that crack propagation is under mixed-mode loading since the ridge interface is at certain inclination angle to the loading. Therefore, the fatigue crack propagation on the interface is influenced not only by the loading and material properties, but the asperity of the interface as well.

In diffusion bonding, it has been accepted that the finer the roughness of the surface to be bonded, and the better the bonding quality will be. However, as mentioned above, the ridge interface can be a resistance to the fatigue crack propagation. So the conclusion of the finer the roughness, the better the joint quality is questionable to similar diffusion bonded joints. Somekawa [16,17] investigated the relationship between surface roughness and diffusion bonding quality of Mg–Al–Zn alloy and AZ31. Joint quality was assessed by the compressive lap shear tests. The results showed that the optimal surface roughness was equal to grain size of material. Although the applicability of this conclusion to other materials needs further experimental verification, it provides us with important information for optimizing the surface roughness according to the service condition (such as loading).

The transgranular crack growth can be seen clearly in Fig. 4(g) ($N = 26\,500$). The main crack A deflected the interface and extended through the grain, forming crack G. Unexpectedly, a new crack I appeared at the crack tip and advanced towards interface. It coalesced with the micro-void when met the interface, Fig. 4(i) ($N = 27\,500$). In subsequent propagation, the main crack deviated the interface and turned to transgranular growth, Fig. 4(j) ($N = 28\,000$), forming a wavy path. An interesting thing during the crack growth was that: the transgranular crack grew no more than 0.05 mm. Then it returned back to the interface. The same phenomenon was also found in Fig. 4(f) and (j).

The crack propagation path in Fig. 4(k) ($N = 28\,500$) was similar to that in Fig. 4(b), in which the crack grew along the symmetric path of the ridge interface. It can be seen from all images in Fig. 4, that the main crack opening displacement became larger as the crack advanced. As the test proceeded, the stress increased due to the decrease of the specimen section, and eventually the instability of crack growth leads to the final fracture.

From the whole process of crack propagation, we can see that the main crack growth follows a wavy path and exhibits multi-path options: transgranular, intergranular or near the interface.

3.2. Fatigue failure mechanism of 316LSS diffusion bonded joints

The micro-void H grew simultaneously as the crack proceeded, shown in Fig. 4(l) ($N = 29\,500$). Its coalescence with the main crack resulted in a fast increase in the growth rate. The phenomenon is very exceptional in the test. Under the magnification 1000×, a number of repeated tests showed that no size and shape change of the micro-voids ahead of the crack was observed as the crack advanced. For example, the micro-void J (Fig. 5(i)) had no any change after 28 000 cycles, even if the grain adjacent to the micro-void J has deformed obviously, shown in Fig. 4(j).

For the joints of dissimilar materials with discrete interfacial micro-voids located ahead of a crack, the mechanisms of interfacial failure have been accounted for by the following way [18–21]: (1) crack initiation at micro-voids, (2) micro-voids growth, (3) coalescence of crack and micro-voids, (4) coalescence of micro-voids and micro-voids. The process repeats until the crack comes into instable growth and fracture occurs. However, for 316LSS/316LSS joints, the micro-voids ahead of the crack were unchanged as the crack proceeded and no coalescence of micro-voids and micro-voids was observed during the repeated tests. Therefore,

the fatigue failure mechanism of similar diffusion bonded joints is different from that of joints of dissimilar materials.

3.3. Analysis of SEM of fatigue fracture surface

Fig. 5 shows the SEM of the fatigue fracture surfaces. In Fig. 5(a), there are obvious four regions on the appearance of fatigue fracture surfaces: A, B, C and D. A is the notch region; B is the transition region of fatigue crack from the parent material to the interface; C is the fatigue crack propagation region and D is the region of overload fracture.

Clear fatigue striations in region B can be seen from the zoom-in image of I, shown in Fig. 5(b). It can also be seen that fatigue striations extend through grooves which formed in diffusion bonding due to the asperity of surface. Fig. 5(c) shows the intersection of the origin of the crack and notch. From this figure, scratches of surface roughness, the origin of the crack initiation and the fatigue striations can be seen clearly. Both the location of the crack initiation and the crack growth direction showed in this figure is consistent with those observed in Fig. 4(a) ($N = 20\,000$).

Fig. 5(d) shows the magnification of overload fracture region. In the latter stage of the fatigue test, obvious necking behavior occurred on the specimen before the final fracture. This can be verified from lots of dimples in Fig. 5(d).

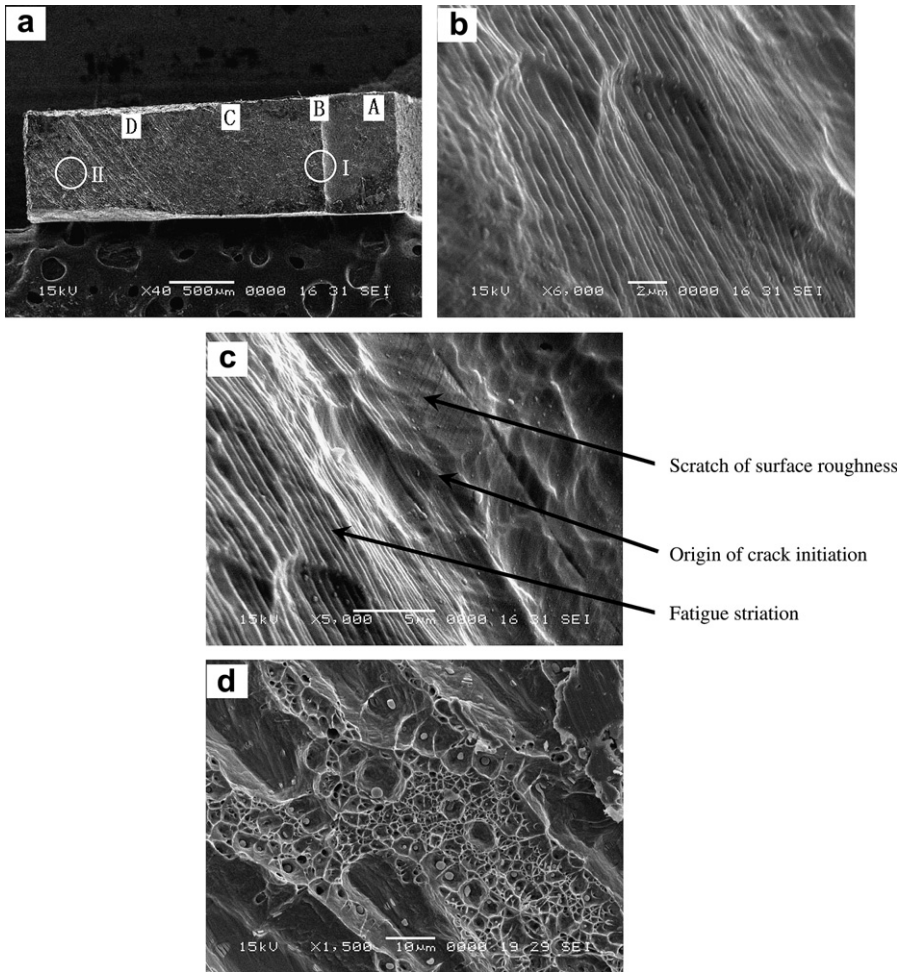

Fig. 5. SEM micrographs of fatigue fracture surface. (a) The whole appearance of fracture surface. (b) Magnification of I, fatigue striations. (c) The intersection of the origin of crack and notch, where the fatigue crack initiates. (d) Magnification of II, dimples in the overload fracture region.

4. Conclusions

(1) Under the magnification 1000×, no size and shape changes of the micro-voids are observed as the crack propagates though the appreciable plastic deformation occurs in grains adjacent to the crack tip, which leads to a great difference of interface failure mechanism between the joints of similar materials and joints of dissimilar materials.
(2) The ridged interface is a resistance to the crack propagation, and thus it reduces the fatigue crack propagation rate to a certain degree. The fatigue crack propagation on the interface is influenced not only by the loading and material properties, but by the roughness of the interface as well.
(3) The matters shown in SEM of fracture surface can be verified by the results of in situ observation. The location of crack initiation and the direction of crack growth in SEM are consistent with those observed in the in situ microfatigue test.

Acknowledgements

The authors are grateful for the supports provided by China Natural Science Foundation (Contract Nos. 50225517, 50475068) and CFKSTIP, Ministry of Education of China (No. 704020). F.Z. would also wish to thank the supports provided by Shanghai Rising-Star Program (No. 05QMX1416).

References

[1] S. Sato, T. Kuroda, T. Kurasawa, J. Nucl. Mater. 233–237 (1996) 940.
[2] T. Takeda, K. Kunitomi, T. Horie, Nucl. Eng. Design. 168 (1997) 11.
[3] G.L. Marois, H. Burlet, R. Solomon, Fusion Eng. Des. 39–40 (1988) 253.
[4] M. Ghosh, D. Samar, P.S. Banarjee, Mater. Sci. Eng. A 390 (2005) 217.
[5] I.S. Batra, G.B. Kale, T.K. Saha, Mater. Sci. Eng. A 369 (2004) 119.
[6] R.H. Vegter, A.T.J.V. Helvoort, G.D. Ouden, J. Adv. Mater. 35 (2003) 17.
[7] R. Polanco, A.D. Pablos, P. Miranzo, Appl. Surf. Sci. 238 (2004) 506.
[8] M. Ghosh, S. Chatterjee, Mater. Sci. Eng. A 358 (2003) 152.
[9] H. Nishi, T. Araki, J. Nucl. Mater. 283–287 (2000) 1234.
[10] H. Nishi, J. Nucl. Mater. 329–333 (2004) 1567.
[11] S. Sato, T. Hatano, T. Kurasawa, J. Nucl. Mater. 258–263 (1998) 265.
[12] G.L. Marois, C. Dellis, J.M. Gentzbittel, J. Nucl. Mater. 233–237 (1996) 927.
[13] Y.H. Lin, Y.C. Hu, C.M. Tsai, Acta Mater. 53 (2005) 2029.
[14] Y. Tanaka, Z.Y. Deng, Y.F. Liu, Acta Mater. 51 (2003) 6329.
[15] S.F. Zhu, Y. Kagawa, M. Mizuno, Mater. Sci. Eng. A 220 (1996) 100.
[16] H. Somekawa, K. Higashi, Mater. Trans. 44 (8) (2003) 1640.
[17] H. Somekawa, H. Hosokawa, H. Watanabe, Mater. Sci. Eng. A 339 (2003) 328.
[18] E.K. Tschegg, H.O.K. Kirchner, M. Kocak, Acta Metall. Mater. 38 (3) (1990) 469.
[19] R.M. Cannon, B.J. Dalgleish, R.H. Dauskardt, Acta Metall. Mater. 39 (9) (1991) 2145.
[20] C. Woeltjen, C.F. Shih, S. Suresh, Acta Metall. Mater. 41 (8) (1993) 2317.
[21] M.R. Turner, A.G. Evans, Acta Mater. 44 (3) (1996) 863.